

# Control-Oriented Modeling of Sheet and Film Processes

Andrew P. Featherstone and Richard D. Braatz

Dept. of Chemical Engineering, 600 South Mathews Avenue, Box C-3, University of Illinois at Urbana-Champaign, Urbana, IL 61801

*Sheet and film processes pose a challenging identification and control problem due to high complexity, poor conditioning, and limited input-output data. The interaction between model accuracy and closed-loop performance is explored for sheet and film processes using a model decomposition in terms of two static orthogonal matrices in series with a diagonal transfer-function matrix. It is shown that the accuracy of the diagonal elements of the transfer-function matrix directly specifies the closed-loop performance achievable by a model-based controller. This motivates the development of a combined identification and control procedure in which the controller is designed to be robust to model inaccuracies quantified during identification. The resulting controller is compared to an industrially accepted controller design method for two examples, including a simulated blown-film process. Based on the theoretical results and simulations, it was concluded that the poor performance often reported for existing industrial sheet and film process-control systems is likely due to signs of the model gains being incorrectly identified.*

## Introduction

Sheet and film processes constitute an industrially important class of structured large-scale systems that include coating, papermaking, and polymer film extrusion processes. Improved control of sheet and film processes can mean significant reductions in material consumption, greater production rates for existing equipment, improved product quality, elimination of product rejects, and reduced energy consumption.

The numerical difficulties associated with handling large-dimensional processes prevent the application of many advanced control algorithms and identification procedures suitable for smaller-scale processes (Braatz et al., 1996). More importantly, large-scale systems are almost always poorly conditioned, and such processes are well known to be difficult to control (Skogestad et al., 1988). This poor conditioning is especially critical for sheet and film processes, for which the quantity of high-quality experimental data is usually extremely limited (Featherstone and Braatz, 1995). These characteristics and experimental constraints lead to difficulty in obtaining acceptable models for control.

Model-based control strategies depend on process characteristics that must be accurately identified in the model, otherwise poor performance or instability may result. The purpose of this investigation is to understand the relationship between the quality of the process model and the resulting closed-loop performance. This problem is studied using a model decomposition in terms of a static input rotation matrix, a diagonal transfer-function matrix, and a static output rotation matrix. Theoretical results and simulations indicate that manipulations should be performed only in directions of the process input vectors corresponding to steady-state gains of the diagonal elements of a transfer-function matrix whose signs have been reliably identified. The accuracies of the steady-state gains are quantified from the input-output data, and a controller is designed to be robust to inaccuracies in the controlled model gains and in the input and output rotation matrices. The improved reliability of the controller is demonstrated by comparison with an industrially accepted control methodology.

The manuscript is organized as follows. First, we provide a brief description of sheet and film processes, focusing on the characteristics relevant for model identification. Second, ex-

Correspondence concerning this article should be addressed to R. D. Braatz.

isting directionality identification techniques are reviewed, with attention to the difficulties in applying these techniques to large-scale sheet and film processes. Third, we discuss model structures appropriate for sheet and film processes, including a model decomposition in terms of two static orthogonal matrices in series with a diagonal transfer-function matrix. It is shown that the accuracy of the diagonal elements of the transfer-function matrix directly specifies the closed-loop performance achievable by a model-based controller. This motivates the development of a combined identification and control procedure in which the controller is designed to be robust to model inaccuracies quantified during identification. The resulting controller is applied to two examples, including a simulated blown-film process.

## Sheet and Film Processes

Sheet and film can be produced as either flat or circular webs (see Figures 1 and 2). Products produced as flat webs (see Figure 1) include newspaper, cardboard, plastic sheets, and bumper stickers. Tubular blown-plastic film is produced as a circular web (see Figure 2) that can be cut to yield a flat film or used in tubular form for bag and sack products. Thin film lines (film thickness less than  $100\ \mu\text{m}$ ) produce products such as laminating, thin shrink, form-and-fill, bag, and general packaging films (Hensen, 1988). Heavy-duty film line products include heavy-duty sack, refuse-sack, heavy-duty shrink, and carrier-bag film (Hensen, 1988). Sheet and film processes typically operate at high speeds, with coating machines as fast as  $6\ \text{m/s}$  (Braatz et al., 1992; Young et al., 1986), paper machines up to  $16\ \text{m/s}$  (Kan, 1987), and stretch film lines up to  $7.6\ \text{m/s}$  (Wigotsky, 1996).

Most sheet and film processes have two main control objectives (see Figure 1). One is the maintenance of the *average* sheet or film thickness, which is referred to as the *machine-direction* (MD) control problem. The other is the maintenance of flat profiles across the machine web, referred to as the *cross-directional* (CD) control problem. Significant CD variations can be present, even when there are no MD variations, resulting in sheets that bulge or will not lie flat when wound into rolls. There exist strong interactions between actuator movements and the resulting sheet profile, making the CD control problem challenging and interesting. Since the MD problem has been extensively studied (Åström et al., 1977; Åström and Wittenmark, 1973; Bialkowski, 1978, 1983; Cegrell and Hedqvist, 1975; Dumont, 1986; Ma and Williams, 1988; Sikora et al., 1984), only the CD problem will be discussed here.

In blown-film extruders, variations in film thickness could arise from imperfections on the die surface, as well as from changes in the physical properties of various polymers used in different extrusion runs. The two types of devices used to adjust the gap thickness in operation are choke bars (restrictor bars) and flexible lips. These devices have a large number of screws or bolts across their width that permit local adjustments (Wigotsky, 1996; Charrier, 1991). Also, thickness variations can be controlled by adjusting the temperature of the polymer melt at the die surface (see Figure 3) (Wigotsky, 1996; Callari, 1990; Hensen, 1988). For blown-film lines, variations in the MD should be less than  $\pm 2\%$  from the average, and CD variations (depending on product) can be  $\pm 3\%$  to

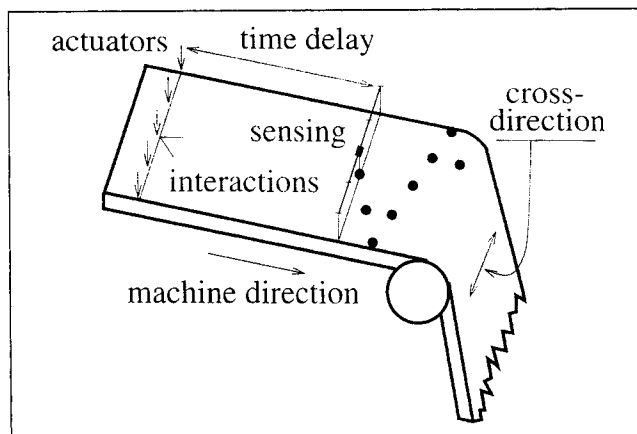


Figure 1. Generic web-forming process (not drawn to scale).

$\pm 15\%$  (Hensen, 1988). Other actuator types common to papermaking are described elsewhere (Braatz et al., 1996).

Actuators used to control the sheet profile are almost always located at evenly spaced points along the cross direction (Braatz et al., 1996). Sensor measurements are taken after some form of processing and are located at a distance down the machine direction from the actuation. Due to their high cost, only a limited number of traversing sensors provide measurements of the sheet or film profile, as illustrated in Figure 1. Since the sheet or film is moving in the machine direction, each sensor measures only a zigzag portion of the sheet or film. In blown-film processes, a measuring device revolves around a film tube, effectively measuring a spiral portion of the film (see Figure 3) (Hensen, 1988). From this limited number of measurements, the entire sheet or film profile (that is, at all sensing locations) must be determined at each sampling time for use by the control algorithm. Paper machines can have up to 100 actuators (Wilhelm, Jr., and Fjeld, 1983) and 500 sensing locations (Kjaer et al., 1994). The number of actuators for blown-film extruders has been reported to be between 45 and 120 (Koop, 1993).

A general characteristic of sheet and film processes is that the measurements are taken at a much slower rate than most of the process dynamics. Also, the dynamics in the mappings of each actuator that move to a downstream sensor reading are approximately the same (Braatz et al., 1996), implying that the primary goal of sheet and film process identification is to correctly capture the steady-state process interactions.

## Previous Research in Directionality Identification

The poorly conditioned character of many sheet and film processes limits the quality of control, since model estimates of gain directionality may be poor. Many researchers have discussed how models with accuracy only in the individual elements of the gain matrix can still have large errors in the gain directionality, resulting in poor or unstable closed-loop performance (Li and Lee, 1994; Jacobsen, 1994; Andersen and Kummel, 1992b; Grosdidier et al., 1985).

Existing identification techniques developed specifically for poorly conditioned processes (Andersen and Kummel, 1992a;

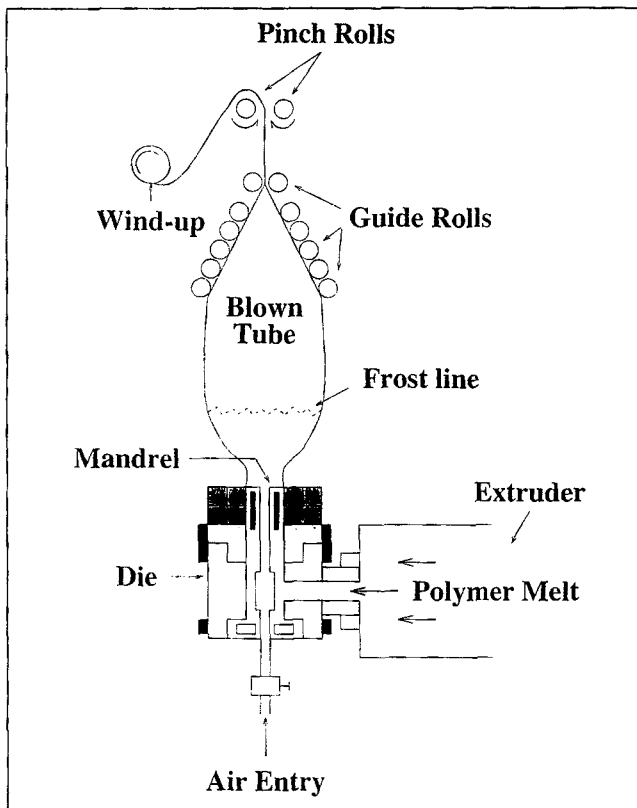


Figure 2. Generic blown-film process (not drawn to scale).

Andersen and Kummel, 1992b; Andersen et al., 1991; Koung and MacGregor, 1993) require much more input-output data than are available for sheet and film processes, and are practically applicable to processes of much smaller dimension. Several researchers (Andersen and Kummel, 1992b; Koung and MacGregor, 1993) have proposed to perform the directionality identification under closed-loop control. However, tuning a controller before performing identification is difficult, especially for poorly conditioned processes. Li and Lee (1994) identify gain directionality by fitting the elements of both the open-loop gain matrix and its inverse. Their ability to more accurately characterize the directionality of poorly conditioned processes occurs at the expense of performing more experiments, and the number of experiments is a strong function of process dimension [e.g., on the order of  $(n-1)^2$  experiments, where  $n$  is the process dimension (Li and Lee, 1994)]. For sheet and film processes, only a limited quantity of experimental data are available from which a model acceptable for control purposes must be identified.

A characteristic of sheet and film processes not addressed in the preceding references is that the measurements are obtained by a small number of traversing sensors. This is the problem of *identification with missing data*, and techniques exist for identifying the nominal model and disturbance characteristics (Jones, 1980; Bergh and MacGregor, 1987). However, these techniques do not provide estimates on the accuracy of the models, nor do they discuss the model accuracy required for effective closed-loop control.

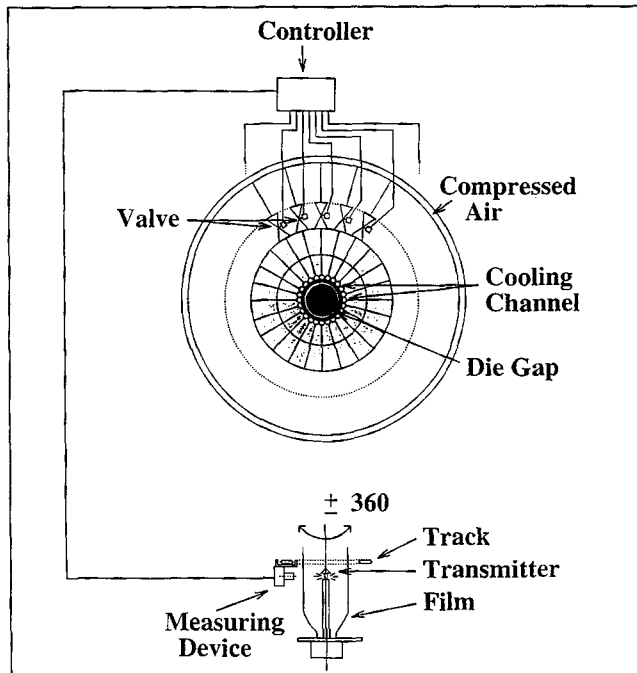


Figure 3. Control of film thickness using cooling air at the die surface (not drawn to scale).

### Model Structures

The quantity of on-line data available for sheet and film processes is low, so that a model with a limited number of parameters must be selected. The traditional model structure for flat-web-forming processes is the Toeplitz symmetric description. For some polymer extrusion applications (Martino, 1991; Callari, 1990), paper machines with neglected edge effects (Laughlin et al., 1993; Wilhelm, Jr., and Fjeld, 1983), and adhesive coating processes (Braatz et al., 1992), the circulant symmetric description can be used. This model structure has more desirable mathematical properties (Featherstone and Braatz, 1995), and is applicable to a wide class of processes of practical importance. Other researchers have chosen to parameterize process signals (e.g., process output, disturbances) and the profile response to each actuator move in terms of a linear combination of basis functions, and to identify the coefficients corresponding to each basis function. Basis functions under study include splines (Halouskova et al., 1993) and discrete orthonormal Chebyshev polynomials, also referred to as Gram or discrete Legendre orthogonal polynomials (Kjaer et al., 1994; Kristinsson and Dumont, 1996).

Many process transfer-function matrices can be decomposed into a structure similar to the singular value decomposition (SVD) (Golub and van Loan, 1983) called the *pseudo-SVD* form (Featherstone and Braatz, 1995; Hovd et al., 1996) with

$$P(s) = U\Lambda(s)V^T, \quad (1)$$

where  $U$  and  $V$  are constant real unitary matrices, but the elements of the diagonal matrix  $\Lambda(s)$  are transfer functions (i.e., can have *phase*), which may be negative and are not necessarily ordered.

A large class of industrially relevant processes can be represented in the pseudo-SVD form. For example, any plant that has the same scalar dynamics  $p(s)$  between each of its manipulated variables and all the measured variables can be written as

$$P(s) = p(s)A, \quad (2)$$

where  $A$  is a constant real matrix. Inserting the SVD of  $A$  and rearranging gives the pseudo-SVD form

$$P(s) = p(s)A = p(s)U\Sigma V^T = U \underbrace{(p(s)\Sigma)}_{\Lambda(s)} V^T. \quad (3)$$

There are many examples of such transfer-function matrices in the chemical process industries, including simplified distillation column models (Skogestad et al., 1988), and every published model of sheet and film processes (Laughlin et al., 1993; Wallace, 1981; Wilkinson and Hering, 1983; Boyle, 1978; Tong, 1976; Wilhelm, Jr. and Fjeld, 1983; Richards, 1982; Cuffey, 1957; Karlsson and Haglund, 1983).

Processes with circulant symmetric descriptions (described earlier) have transfer-function matrices of the form

$$C(s) = \begin{bmatrix} c_1 & c_2 & \cdots & c_{m-1} & c_m & \cdots & c_m & c_{m-1} & \cdots & c_2 \\ c_2 & c_1 & c_2 & \cdots & c_{m-1} & c_m & \cdots & \vdots & \vdots & \vdots \\ \vdots & c_2 & c_1 & c_2 & \cdots & c_{m-1} & \cdots & \vdots & \vdots & c_{m-1} \\ c_{m-1} & \vdots & c_2 & c_1 & c_2 & \cdots & \cdots & \vdots & \vdots & c_m \\ c_m & c_{m-1} & \vdots & c_2 & \vdots & \vdots & \vdots & c_{m-1} & c_m & \vdots \\ \vdots & c_m & c_{m-1} & \vdots & \vdots & \vdots & c_2 & \vdots & c_{m-1} & c_m \\ c_m & \vdots & \vdots & \vdots & \cdots & c_2 & c_1 & c_2 & \vdots & c_{m-1} \\ c_{m-1} & \vdots & \vdots & \vdots & c_{m-1} & \cdots & c_2 & c_1 & c_2 & \vdots \\ \vdots & \vdots & \vdots & \cdots & c_m & c_{m-1} & \cdots & c_2 & c_1 & c_2 \\ c_2 & \cdots & c_{m-1} & c_m & \cdots & c_m & c_{m-1} & \cdots & c_2 & c_1 \end{bmatrix}, \quad (4)$$

$n \times n$

where each  $c_j$  is a transfer function. All circulant symmetric transfer-function matrices can be diagonalized by the real Fourier matrix [details in (Featherstone, 1997, chap. 4)]

$$C(s) = R\Lambda(s)R^T. \quad (5)$$

The decomposition matrix  $R$  depends only on the process dimension and not on localized physical phenomena. This decomposition can be used for any circulant symmetric sheet and film process. An additional property that can be exploited to simplify controller synthesis is that only  $(n+1)/2$  (for  $n$  odd) or  $(n/2)+1$  (for  $n$  even) of the diagonal elements  $\Lambda_{ii}(s)$  are distinct (Hovd et al., 1996).

### Model Requirements

One of the goals of this investigation is to gain insight as to which process characteristics must be extracted for providing

adequate closed-loop performance. To do this, in this section we will assume that the process can be placed in pseudo-SVD form (Eq. 1), and that the orthogonal matrices  $U$  and  $V$  in Eq. 1 are exactly known. The latter assumption will be true for circulant symmetric processes (Eq. 4), in which the orthogonal matrices  $U=V=R$  can be computed *before the experimental data are collected*. In the next section, we describe how to design controllers to be robust to inaccuracies in  $U$  and  $V$ , as would occur, for example, for flat-web processes that have edge effects.

Consider a closed-loop system with the standard feedback controller as shown in Figure 4. Hovd et al. (1996) have shown that for pseudo-SVD processes (Eq. 1), controllers of the form

$$K(s) = V\Lambda_K(s)U^T \quad (6)$$

(referred to as *SVD controllers*) provide optimal performance for a variety of norms (e.g.,  $H_2$ ,  $H_\infty$ ), under mild technical conditions. The optimality is true even for the case where model inaccuracies are represented and the performance is measured in a "worst-case" sense [see (Morari and Zafiriou, 1989; Skogestad and Postlethwaite, 1996) for thorough de-

scriptions of how model uncertainties and worst-case performance measures are addressed]. Given the relatively slow speed of measurements and manipulations compared to the speed of the rest of the process dynamics, the most important

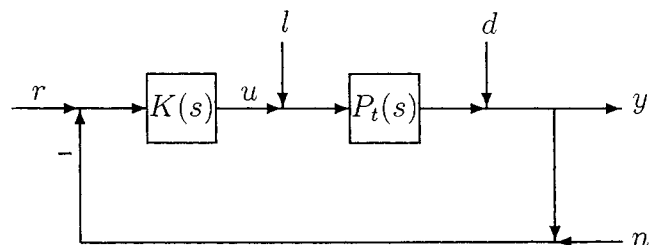


Figure 4. Standard feedback control system.

The manipulated variable is  $u$ , the process output is  $y$ , the setpoint is  $r$ , the measurement noise is  $n$ , and the disturbances are  $d$  and  $l$ .

performance specification for sheet and film processes is zero steady-state error (Braatz et al., 1966). For a stable plant to have zero steady-state error, the final value theorem implies that the controller must have an integrator ( $1/s$ ) in each channel. A SVD controller with integral action in all channels, while having no poles in the open right half plane, will be referred to as an *integral SVD controller*. The performance and robustness characteristics of the SVD controller and the requirement of integral action motivate the following result concerning the gain identification requirements for pseudo-SVD processes.

**Theorem 1.** Consider a closed-loop system without actuator limitations as shown in Figure 4. Assume the true plant [ $P_t(s)$ ] and a model of the plant [ $P_m(s)$ ] are stable proper rational transfer functions that are of the pseudo-SVD form [ $P_t(s) = U\Lambda_t(s)V^T$  and  $P_m(s) = U\Lambda_m(s)V^T$ ]. Then an integral SVD controller designed to stabilize  $P_m(s)$  will also stabilize  $P_t(s)$  only if  $\Lambda_{t,ii}(0)/\Lambda_{m,ii}(0) > 0$ , for all  $i$ . Furthermore, there exists an integral SVD controller that stabilizes both  $P_m(s)$  and  $P_t(s)$  and continues to do so with arbitrary detuning of its single-loop gains ( $\Lambda_{K,ii}(0)$ ) if  $\Lambda_{t,ii}(0)/\Lambda_{m,ii}(0) > 0$ , for all  $i$ .

If any of the true process gains  $\Lambda_{t,ii}(0)$  is equal to zero, then there does not exist a nonsingular integral controller that stabilizes the unconstrained closed-loop system (Campo and Morari, 1994). If none of the true process gains is exactly equal to zero, then Theorem 1 implies that an integral SVD controller exists that stabilizes both the model and the true process if each identified model gain  $\Lambda_{m,ii}(0)$  has the same sign as the corresponding process gain of the true process  $\Lambda_{t,ii}(0)$ . Furthermore, these sign conditions must hold for *any* model-based integral SVD controller to stabilize the true process. Relationships between Theorem 1 and other results in the literature are described elsewhere (Featherstone, 1995). The proof of Theorem 1 is given in the Appendix.

For a process without actuator limitations, an integral SVD controller whose design is based on a model with inaccurate signs of its steady-state gains will cause an unstable closed-loop response. Since sheet and film processes (like all real systems) have constraints on their actuator moves, the vector of manipulated variables for such a controller will grow in magnitude until the actuator moves become limited, irrespective of how small the disturbances are that enter the system. Although Theorem 1 does not imply that any *non-SVD* integral controller whose design is based on a model with inaccurate signs of its steady-state gains will destabilize the closed-loop system, such destabilization will tend to occur [see (Featherstone, 1997) for a more detailed development], as will be illustrated in the Examples section.

## Coupling Identification and Control

The poor conditioning of sheet and film processes makes it difficult to reliably identify the signs of all of the process gains  $\Lambda_{t,ii}(0)$  from the limited input-output data usually available for sheet and film processes (this will be illustrated using rigorous statistical analysis in the next section). This motivates the idea of designing the controller to only perform manipulations in directions that correspond to model gains  $\Lambda_{m,ii}(0)$  whose signs are known with confidence (these directions are the corresponding columns  $V_i$  of the process input rotation matrix  $V$ ). Manipulations in directions corresponding to

process gains whose signs may be incorrectly identified may lead to poor closed-loop performance. These considerations, and the proven robustness and optimality properties of the SVD controller (Eq. 6), motivate the following coupling between the identification procedure and the controller design.

## Identification

The input-output data are collected and used to statistically fit a model for the process dynamics  $g(s)$  (in Eq. 3) and the steady-state-process interaction matrix  $P_m(0)$ . The scalar dynamics for sheet and film processes are well-described as being first-order plus time delay (the approach can be generalized), and are scaled so that  $g(0) = 1$ . The process model gains  $\Lambda_{m,ii}(0)$  are computed by taking a matrix decomposition of the steady-state interaction matrix  $P_m(0) = U\Lambda_m(0)V^T$  estimated from the input-output data. This results in

$$P_m(s) = \frac{e^{-\theta s}}{\tau s + 1} P_m(0) = \frac{e^{-\theta s}}{\tau s + 1} U\Lambda_m(0)V^T = \frac{e^{-\theta s}}{\tau s + 1} \sum_{i=1}^n \Lambda_{m,ii}(0)U_iV_i^T. \quad (7)$$

## Controller design

Basic statistical analysis is used to compute confidence intervals for each  $\Lambda_{m,ii}(0)$  (Brunk, 1965; Devore, 1982). The SVD controller is designed to only make manipulated variable moves in the directions  $V_i$  corresponding to gains  $\Lambda_{m,ii}(0)$  that are known with confidence. The confidence intervals describe the accuracy of each controlled gain, and are used to design a controller robust to the potential gain variations.

The robust-controller design procedure, described in detail elsewhere (Hovd et al., 1996; Braatz and VanAntwerp, 1996b) is summarized below. First, standard block-diagram algebraic manipulations [either by hand (Morari and Zafiriou, 1989; Skogestad and Postlethwaite, 1996) or using off-the-shelf programs (Balas et al., 1992; Chiang and Safonov, 1992; Russell and Braatz, 1996; Russell et al., 1997)] are used to construct the standard uncertain system representation in Figure 5. The test for robust stability is that

$$\sup_{\omega} \mu\{F_i[N(j\omega), K(j\omega)]\} < 1, \quad \forall \omega, \quad (8)$$

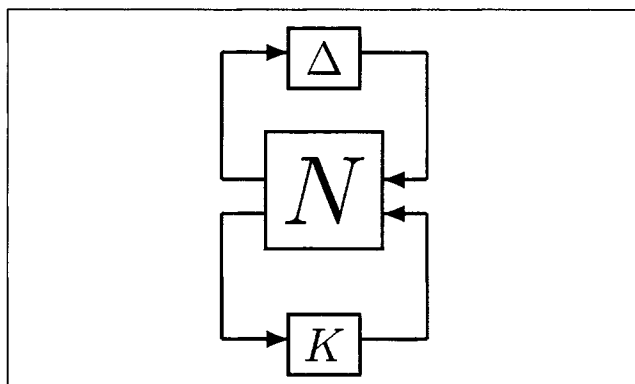


Figure 5. Uncertain system representation.

where  $F_l(N(j\omega), K(j\omega))$  is the lower linear fractional transformation (LFT) between  $N$  and  $K$ , and  $\mu$  is the robustness margin [for background on robustness analysis, see Doyle (1982); Safonov (1982); Morari and Zafiriou (1989); Skogestad and Postlethwaite, (1996)]. It is important to note that the lefthand side of Eq. 8 is computable from the controller  $K$ , the plant  $P$ , and the uncertainty description. In general, robustness margin computations are computationally expensive for processes of high dimension (Braatz et al., 1994; Braatz, 1996). However, with pseudo-SVD processes, the dimension of the problem can be reduced for a broad class of realistic uncertainty descriptions, including descriptions that capture inaccuracies in the process input and output rotation matrices  $U$  and  $V$ , which would represent structural mismatch, for example, due to edge effects [for details see Braatz and Van Antwerp (1996b)]. The robustness margin for pseudo-SVD processes can be computed as

$$\mu\{F_l[N(j\omega), K(j\omega)]\} = \max_i \{\mu\{F_l[N^i(j\omega), \Lambda_{K,ii}(j\omega)]\}\}, \quad (9)$$

where  $N^i$  corresponds to a single-input, single-output (SISO) robust controller design problem for each controlled gain  $\Lambda_{m,ii}(s)$ . This decouples the design problem for  $K(s)$  into *independent* design problems for each  $\Lambda_{K,ii}(s)$ . The controller  $\Lambda_{K,ii}(s)$  for each SISO problem can be designed by any robust-controller method; we suggest to use IMC tuning (Morari and Zafiriou, 1989):

$$\Lambda_{K,ii}(s) = \frac{1}{\Lambda_{m,ii}(0)} \cdot \frac{\left(1 + \tau_D s + \frac{1}{\tau_I s}\right)}{\tau_{F,i} s + 1} \cdot \frac{2\tau + \theta}{2(\lambda_i + \theta)}$$

for  $\Lambda_{m,ii}$  known with confidence (otherwise,  $\Lambda_{K,ii}(s) = 0$ ),

$$(10)$$

with

$$\tau_I = \tau + \frac{\theta}{2}; \quad \tau_D = \frac{\tau\theta}{2\tau + \theta}; \quad \tau_{F,i} = \frac{\lambda_i\theta}{2(\lambda_i + \theta)}.$$

The SISO controllers  $\Lambda_{K,ii}(s)$  are stacked up as the diagonal elements of a matrix  $\Lambda_K(s)$ , with the overall SVD controller computed from

$$K(s) = V\Lambda_K(s)U^T. \quad (11)$$

The IMC tuning parameters  $\lambda_i$  are selected as fast as possible while maintaining stability for all variations in model gains and input/output rotation matrices. As recommended by Morari and Zafiriou (1989), each  $\lambda_i$  also has a lower bound of  $1.7\theta$  to prevent large overshoots in the presence of time delays. Any of the well-established multivariable antiwindup procedures can be used to deal with the constraints (Åström and Wittenmark, 1984; Campo and Morari, 1990; Mhatre and Brosilow, 1996; Zheng et al., 1994). Constraint handling may be unnecessary for many sheet and film processes, since directions corresponding to low steady-state gains  $\Lambda_{m,ii}(0)$  are

not manipulated by the SVD controller, and designing the controller to be robust tends to prevent overly large dynamic excursions in the manipulated variables. This is illustrated in the following examples.

## Examples

The following examples illustrate the relationship between process identification and the controller design. To simplify the concepts being demonstrated, a  $5 \times 5$  circulant symmetric process is studied first. Second, the technique is applied to a large-scale blown-film process. While the theoretical results hold for more general pseudo-SVD processes, for brevity only circulant symmetric processes are simulated here.

### 5 × 5 Example

For the first example, the true process transfer-function matrix  $P(s)$  is taken as

$$P_t(s) = g(s)P_t(0) = \frac{e^{-\theta s}}{\tau s + 1} \begin{bmatrix} 1 & 0.9 & 0.7 & 0.7 & 0.9 \\ 0.9 & 1 & 0.9 & 0.7 & 0.7 \\ 0.7 & 0.9 & 1 & 0.9 & 0.7 \\ 0.7 & 0.7 & 0.9 & 1 & 0.9 \\ 0.9 & 0.7 & 0.7 & 0.9 & 1 \end{bmatrix}, \quad (12)$$

where  $\theta = \tau = 1$ . The condition number of the process is  $\kappa[P_t(j\omega)] = 178$  for all frequencies, which is large, suggesting potential identification and control problems. The focus will be on the identification of the steady-state interaction matrix  $P_t(0)$ , since the scalar dynamics do not pose any special robustness or performance difficulties.

*Identification.* During identification, the measured process output at steady state  $y_m$  is assumed to be given by

$$y_m = P_t(0)u + v, \quad (13)$$

where  $u$  is the actuator input move and  $v$  represents zero-mean Gaussian measurement noise. In the standard industrial experiment (called a "bump test"), the open-loop response is measured for a step in one of the manipulated variables. This defines the process input as  $u = \alpha e_1$ , where

$$e_1 = \begin{bmatrix} 0 \\ 0 \\ 1 \\ 0 \\ 0 \end{bmatrix}. \quad (14)$$

To prevent excessive process upsets during experimental data collection, constraints are imposed on the process inputs and outputs. For sheet and film processes the constraints on the manipulated variables at each time instance are usually of the forms (Braatz et al., 1996; Braatz and VanAntwerp, 1996a; Chen and Wilhelm, 1986)

$$\begin{aligned} u_l \leq u_i \leq u_h, & \quad (\text{min-max constraint}) \\ -l_b \leq u_{i-1} - 2u_i + u_{i+1} \leq l_b & \quad (\text{2nd-order bending} \\ & \quad \text{moment constraint}). \end{aligned} \quad (15)$$

As discussed in Laughlin et al. (1993), the constraints are functions of the flexibility of the slice (or die) lip, and the number of allowable actuator locations. Tighter control of the cross-directional profile requires more actuator locations with more flexible slice lips. However, slice lips made of materials that are very flexible may not be as durable under the operating conditions as would stronger, less flexible materials. Therefore a trade-off is required, and certain slice-lip designs may be applicable to some processes and operating conditions and not to others. Other manipulations, such as steam sprays or cooling air jets, can be substantially less constrained.

For this example, first it will be assumed that  $-u_l = u_h = 1$  and  $l_b = 2$ , which is applicable for a rigid slice lip. These conditions are described by constraint set 1 (CS-1). The effects of weaker constraints will be investigated, allowing for more flexible slice lips with larger operating regions. Constraint set 2 (CS-2) is described by letting  $u_h = 10$  and  $l_b = 10$ , which are weaker constraints than CS-1. For the identification experiments,  $\alpha$  is usually selected as large as possible without violating any of the constraints (here, it is assumed that the output constraints indicate that the largest allowable weight is  $\alpha = 1$ , which is also appropriate for CS-1). Then the output to the single-step input experiment is

$$y_m = \begin{bmatrix} 0.7 \\ 0.9 \\ 1.0 \\ 0.9 \\ 0.7 \end{bmatrix} + v. \quad (16)$$

Because a substantial fraction of the noise occurring in sheet and film processes is associated with the sensor, the measurement noise in each sensing location is considered to be independent. The variance is assumed to be 0.04, which is a reasonable value for many sheet and film processes. It is industrial practice to repeat the bump tests several times to reduce the effects of noise. Simulated identification experiments consisted of five step input tests, and the process parameters were calculated using least squares. The estimated interaction parameters  $c_i(0)$  (see Eq. 4) and the steady-state plant  $\Lambda_{t,ii}(0)$  and model gains  $\Lambda_{m,ii}(0)$  from a sample data set are shown in Table 1.

The results show that the signs of the process gains can be identified incorrectly with only very small element-by-element errors in the estimated process model. For the sample data set, the sign of the smallest process gain  $\Lambda_{m,33}(0)$  is incorrect (see the last column of Table 1), even though the maximum error is less than 9% for any of the estimated parameters  $c_j(0)$ .

The next step is to determine which signs of the identified gains are known with confidence, based on the experimental data. The confidence interval of each gain is calculated using

**Table 1. Data Set from a Simulation Experiment with Five Open-Loop Step-Response Tests on the Process  $P_i$  Defined in Eq. 12 with Measurement Noise**

	$c_1(0)$	$c_2(0)$	$c_3(0)$	$\Lambda_{11}(0)$	$\Lambda_{22}(0)$	$\Lambda_{33}(0)$
Exp. Data	1.0900	0.9013	0.6878	4.2683	0.5342	0.0568
$P_i(0)$	1.0000	0.9000	0.7000	4.2000	0.4236	-0.0236

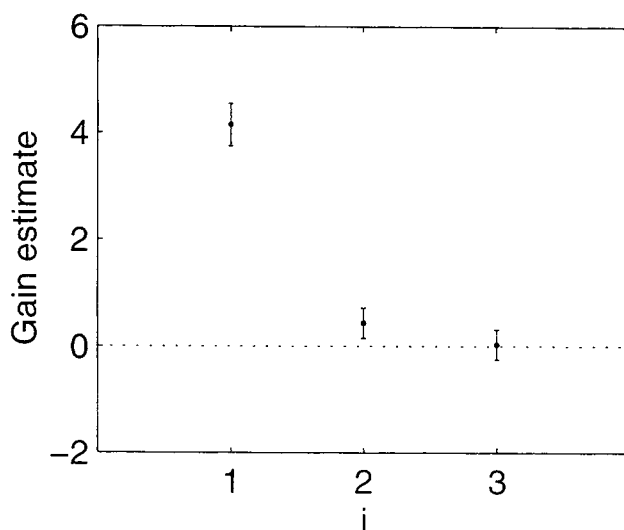


**Figure 6. 95% confidence intervals for each model gain  $\Lambda_{m,ii}$  from experimental data for the  $5 \times 5$  example.**

the estimated noise variance (this is known in practice), the number of bump tests, the known input  $u$ , and the measured output  $y_m$ . If the confidence interval includes zero, then the sign is not known with confidence [although not shown here for brevity, this procedure can be posed rigorously in terms of hypothesis testing, as discussed in detail in (Featherstone, 1997, chap. 5)]. Figure 6 shows the 95% confidence interval for each gain for the sample data set.

Figure 6 indicates that the sign of the third process gain  $\Lambda_{m,33}(0)$  is not known with confidence, since the radius of the interval is larger than the absolute value of the gain. Inspection of the confidence interval corresponds to a hypothesis test with a 97.5% level of significance that the sign of the gain is identified correctly. If fact, rigorous statistical analysis indicates that there is only a 57% probability of correctly identifying the sign of this gain.

**Controller Synthesis.** The SVD controller was designed to minimize the effect of output disturbances  $d$  on the controlled variable  $y$  (see Figure 4), while being robustly stable to actuator and model gain uncertainties [sensor uncertainties were ignored in this example because they usually have a much smaller effect on the robustness of the closed-loop system than actuator uncertainties (Skogestad et al., 1988)]. The robust stability requirement corresponds to the block diagram for the process with uncertainty blocks, as shown in Figure 7 [see (Morari and Zafiriou (1989) and Skogestad and Postlethwaite (1996) for background on the use of  $\mu$  for robustness analysis)]. The uncertainty associated with each actuator (this, for example, could result from stiction or motor wear) is normally assumed to be independent of the other actuators, which corresponds to a diagonal perturbation block  $\Delta_I$ . Instead  $\Delta_I$  is represented as being full to account for inaccuracies in the input rotation matrix  $R$  (in general, this uncertainty description could account for inaccuracies in any input rotation matrix  $V$ ), and for structural mismatch, for example, due to the process not having exactly a circulant symmetric structure due to edge effects. The actuator uncertainty weight  $W_f(s) = 0.3(0.1s + 1)/(0.02s + 3)I$  allows 10%

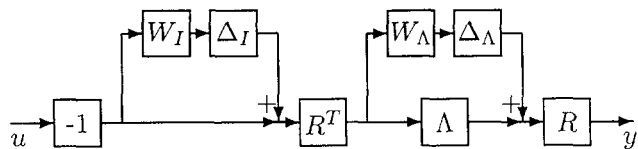


**Figure 7. Process with input and gain uncertainty weights.**

steady-state error in manipulated variable movements and 150% error at high frequencies, with corner points at  $\omega = 10$  and  $\omega = 150$ . The uncertainty in gain  $\Delta_\Lambda$  is diagonal, with  $W_\Lambda$  based on the radii of the confidence intervals in Figure 6. The full  $N(s)$  matrix (as shown in Figure 5), constructed from the block diagram of the process (Figure 7), is given by

$$N(s) = \begin{bmatrix} 0 & 0 & -W_I(s) \\ W_\Lambda R^T & 0 & -W_\Lambda R^T \\ R\Lambda_m(s)R^T & R & -R\Lambda_m(s)R^T \end{bmatrix} \quad (17)$$

and  $\Delta = \text{diag}\{\Delta_I, \Delta_\Lambda\}$ . The controller design problem can be decoupled into the associated SISO subproblems, as discussed in the previous section, with  $N^i$  given as

$$N^i(s) = \begin{bmatrix} 0 & 0 & -W_{I,ii}(s) \\ W_{\Lambda,ii} & 0 & -W_{\Lambda,ii} \\ \Lambda_{m,ii}(s) & 1 & -\Lambda_{m,ii}(s) \end{bmatrix} \quad (18)$$

This allows the SISO controller  $\Lambda_{K,ii}(s)$  for each controlled process gain  $\Lambda_{m,ii}(s)$  to be designed independently.

Based on the identification results, three nonzero SISO controllers  $\Lambda_{K,ii}(s)$  are designed based on the two reliably identified gains. The uncertainty weights used for the computations are  $W_{\Lambda,11} = 0.3920$  and  $W_{\Lambda,22} = W_{\Lambda,55} = 0.2772$ . The IMC parameter for each SISO controller  $\Lambda_{K,ii}(s)$  was tuned as fast as possible while achieving robust stability, while satisfying the lower bound of  $\lambda_i = 1.7\theta$  (in fact, for this example each  $\lambda_i$  was equal to  $1.7\theta$ ). The overall SVD controller is constructed as in Eq. 11, and will only perform manipulations in the three directions corresponding to the two reliably identified gains (one of the gains has two directions corresponding to it). The value for  $\mu$  for the entire system based on the identified model is 0.5416, which indicates that the closed-loop system is stable for the actuator and model gain variations.

**Time-domain Simulations.** The SVD controller is compared to a controller designed with the Quadratic Penalty Function (QPF) method (Chen and Wilhelm, 1986). This model-based method uses time-varying control penalty weights to minimize the performance objective while satisfying actuator constraints. The QPF method often has similar performance to model predictive control (MPC), but is less computationally intensive. For these reasons, the method is widely applied to industrial sheet and film processes (Chen and Wilhelm, 1986). Our implementation of the method may not correspond exactly to the latest version of the QPF method, as the original manuscript describing the method is somewhat sketchy (Chen and Wilhelm, 1986), and the details

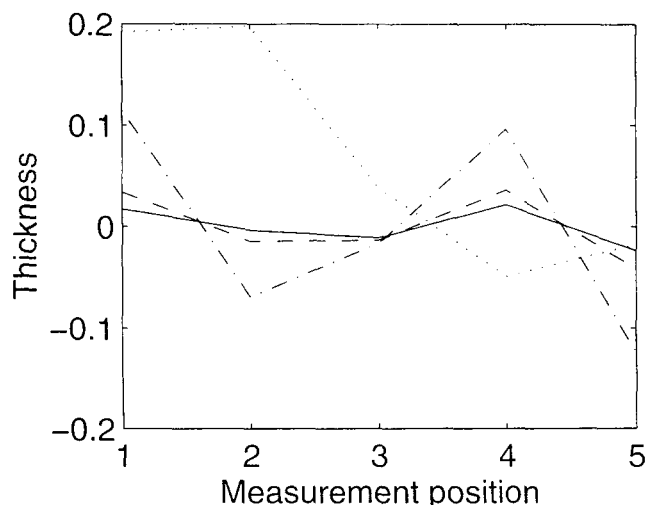


**Figure 8. Steady-state controlled-variable profiles using the SVD and QPF controllers for the  $5 \times 5$  example.**

SVD, model 1 (—); QPF at CS-1 (---); QPF at CS-2 (-.-.); initial disturbance (···).

of the current version are proprietary (this algorithm was owned by ABB as of publication). The main conclusions drawn from the simulations using the QPF control algorithm do not depend on the details of the implementation of the algorithm.

Figure 8 shows the final steady-state profiles after control from a random disturbance using the QPF method under the two constraint sets and the SVD controller. The time-domain response profiles for the process using the QPF controllers at the two constraint sets are shown in Figures 9 and 10, and the SVD controller is shown in Figure 11.

The effect of the misidentified process gain (see Table 1) on the performance of the QPF controller is clearly seen in the responses shown in Figures 9 and 10. Since the final profile response under CS-2 is worse than under CS-1 (see Table

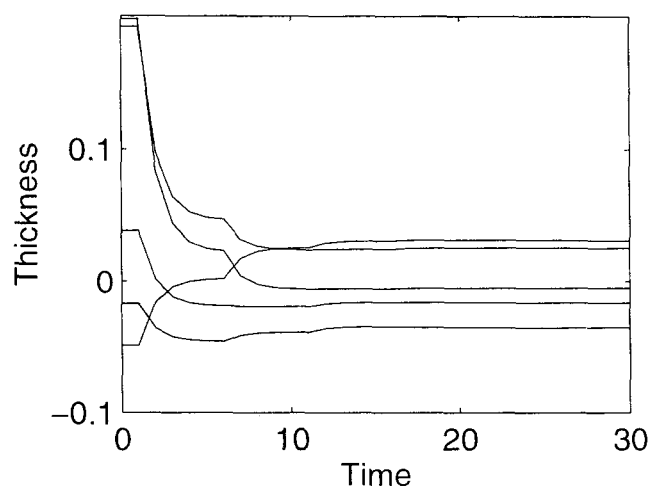


**Figure 9. Time-domain profile response using the QPF controller under Constraint Set 1 for the  $5 \times 5$  example.**



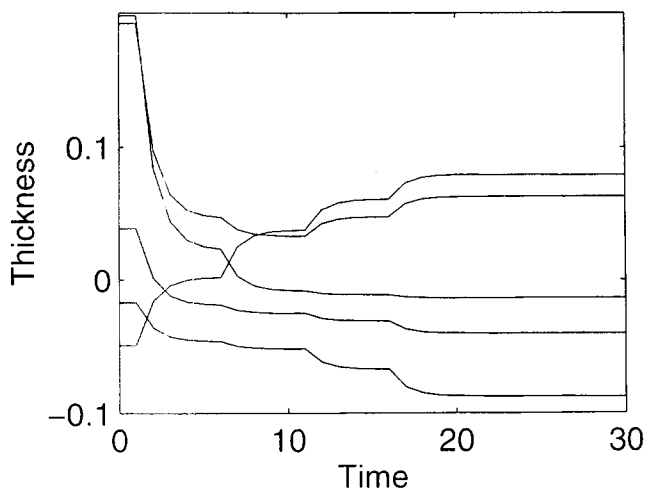


**Figure 10. Time-domain profile response using the QPF controller under Constraint Set 2 for the  $5 \times 5$  example.**

2 and Figure 8), it is apparent that the controller forces the manipulated inputs into directions that give poor final responses, which are larger with the weaker constraints.

The SVD controller design performs input moves only in directions corresponding to the accurately identified gains and avoids the directions corresponding to the misidentified gain (see Figure 11). Only the projection of the disturbance in the controlled direction goes to zero (due to the integral control), which leaves some offset. The final profile resulting from the SVD control response has a smaller standard deviation than the final profiles from either QPF control response. The manipulated variable moves for the SVD controller easily satisfy the constraints, with a maximum deviation of 0.3220 and a maximum second-order bending moment of 0.4669.

We would like to stress that the poor performance of the QPF method designed based on a poorly identified model (see Figure 8) is not due to the QPF controller being tuned over aggressively (Figures 9–11 show that the QPF controllers have a similar speed of response as the SVD con-

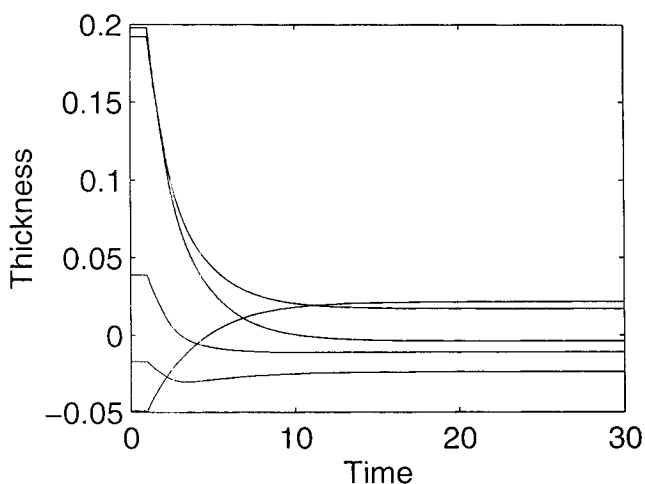


**Figure 11. Time-domain profile response using the SVD controller for the  $5 \times 5$  example.**

**Table 2. Standard Deviation ( $\sigma$ ) of the Initial Disturbance Profile and Steady-state Profiles after Control for the  $5 \times 5$  Example**

	Initial Disturbance	SVD	QPF at CS-1	QPF at CS-2
$\sigma$	0.1161	0.0191	0.0338	0.1038

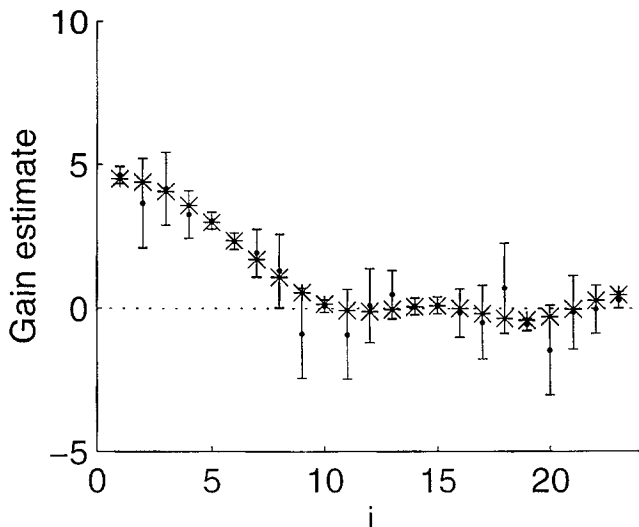
trollers). The poor performance of the QPF method is not due to a deficiency in the QPF controller-design method. If the QPF controller was based on a model that accurately identified the signs of all the gains, the controller would perform well, and weaker constraints would result in improved disturbance rejection. In this example, however, there is only a 57% probability of correctly identifying the sign of the third gain. It is straightforward to extend the results of the section on model requirements to show that model-inverse-based SVD controllers and simple PI controllers all give poor performance if designed to control a manipulated variable direction corresponding to a process gain with an incorrectly identified sign (Featherstone, 1997). The poor performance of the industrially accepted QPF method reinforces the results in the section on model requirements, that model-based controller design methods have difficulty controlling the process effectively if the model does not have the correct signs of the process gains.

### Blown-film example

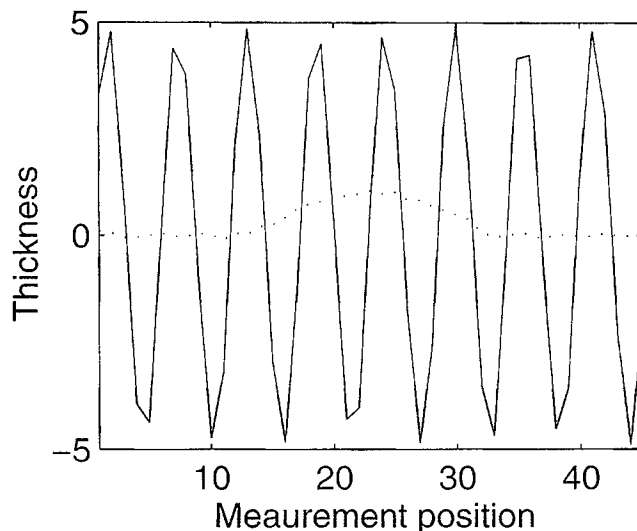
The second example to be considered was a blown-film plastic extruder with 45 actuator and measurement locations. Since the actuator die is circular, the circular symmetric process description is applicable. The steady-state interaction matrix was assumed to have seven parameters, and the noise level was chosen to give realistic signal-to-noise ratios for such machines. For this example, the measurement noise in each sensing location was again considered to be independent and have a variance of 0.04. Following a procedure suggested by Heaven et al. (1993), the step input was performed in a number of actuator locations that are separated so that the resultant bump response profiles are expected not to overlap. Although other input designs could have been chosen [see Featherstone (1997); Van den Hof and Schrama (1995) for discussions of this and related topics], the industrial-standard bump test was selected so that the results of this article would be more closely related to current industrial practice. The process model was identified with five bump tests and the values of the process gains were calculated using least squares.

Figure 12 shows the confidence interval associated with each (distinct) identified process gain, as well as the values of the gains for the true process. Based on the criteria that the interval must not include zero, thirteen of the twenty-three distinct gains were not known with confidence. Of these thirteen, six were actually identified incorrectly. The problem was then reduced to designing SISO controllers for the remaining ten gain directions. The actuator uncertainty description and robust controller design procedure of the first example were used, that is, each SISO controller was chosen to be IMC-PID, and the tuning parameter  $\lambda_i$  was optimized for each subproblem, while satisfying the suggested lower bound.

The full SVD controller was then tested against the QPF method at CS-1 and CS-2. The final profile responses at each



**Figure 12.** Plant gains  $\Lambda_{t,ii}$  (shown using \*) and the 95% confidence intervals for each model gain  $\Lambda_{m,ii}$  from experimental data for the blown-film example.



**Figure 14.** Steady-state controlled-variable profile using the QPF at CS-2 (—) controller for the blown-film example with initial disturbance (···).

arrangement location after control are shown in Figures 13 and 14 with the initial disturbance, and the standard deviations of all the profiles are listed in Table 3.

The effect of the misidentified process gains (see Figure 12) on the performance of the QPF controller is clearly seen in the responses shown in Figures 13 and 14. The response is similar to, yet more extreme than, the response seen for the  $5 \times 5$  example, where there was only one misidentified gain. Again, the QPF model gives poor performance when the model is identified incorrectly. The severity of the response is limited by the constraints. The profile response in Figure 14 is not locally asymptotically stable, but remains bounded because the inputs are bounded by the constraints. For a real blown-film extruder, the response of the QPF controller in

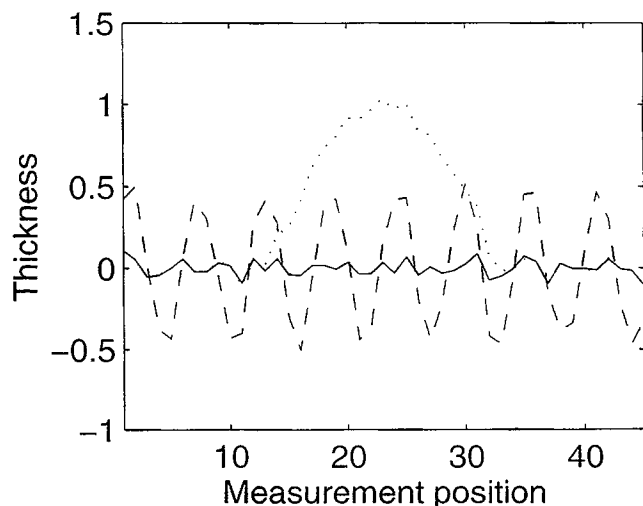


**Figure 13.** Steady-state controlled-variable profiles. SVD (—) and QPF at CS-1 (---) controllers for the blown-film example with initial disturbance (···).

Figure 14 (and possibly in Figure 13) would cause the film to break. Ideally, weakening the constraints should lead to better control, but this will only happen if the controller is based on a sufficiently accurate model. The QPF controller under the weaker constraints yields a worse performance than would have been obtained without the controller. The poor performance is similar to the results from the control system audits reported by Białkowski (1986). Here, the poor performance is a result of the inaccurate model violating the model requirements, and not due to a specific deficiency in the QPF design method. *It is the authors' opinion that the poor performance often reported for industrial sheet and film process control systems is most likely due to the signs of the model gains being incorrectly identified.*

The effect of the misidentified gains is not so apparent in the response due to the SVD controller design (Figure 13). Since the SVD controller does not perform control moves in any of the directions that were inaccurate, the model requirements are satisfied for each controlled direction. The performance limitation is specified by the number of accurately known gains. If the model is improved, then the control would improve. As with the  $5 \times 5$  example, the inputs generated by the SVD controller (figure not shown for brevity) easily satisfies the constraints with a maximum deviation of 0.2449 and a maximum second-order bending moment of 0.0654.

A few final comments are in order. That processes of high dimensionality tend to be poorly conditioned is well known to industrial control engineers (Braatz, 1995), and can be proved using the statistics of large matrices (Braatz, 1997).

**Table 3.** Standard Deviation ( $\sigma$ ) of the Initial Disturbance Profile and Steady-state Profiles after Control for the Blown-Film Example

	Initial Disturbance	SVD	QPF at CS-1	QPF at CS-2
$\sigma$	0.3847	0.0488	0.3642	3.5069

This implies that there is a 50% probability of incorrectly identifying the sign of a gain (or a large number of gains) for a large-scale process. The problem is especially acute for sheet and film processes, for which a limited quantity of experimental data can be collected, and the measurement noise is often high relative to the magnitude of the profile measurement. As such gains cannot be controlled reliably, the controller should not attempt to control in the directions associated with these gains. This implies that there is an inherent performance limitation for large-scale processes that cannot be ignored during the identification and controller design procedure.

## Conclusions

The interaction between model accuracy and closed-loop performance was explored for sheet and film processes using a model decomposition in terms of a static input rotation matrix ( $V$ ), a diagonal transfer-function matrix ( $\Lambda_m(s)$ ), and a static output rotation matrix ( $U$ ). Theoretical results and simulations indicated the importance of only performing manipulations in directions of the process input vectors ( $V_i$ ) corresponding to steady-state gains whose signs have been reliably identified. The SVD controller is designed to be robust to inaccuracies in the controlled-model gains and in the input and output rotation matrices (the examples considered the case with potential inaccuracies in the input rotation matrix). The performance of the SVD controller was compared to that of the industrially accepted QPF controller design method. While attempting to control in all directions was shown to result in poor performance, the SVD controller provided consistently good results. Furthermore, the simulation examples suggested that constraint handling may be unnecessary for many sheet and film processes when the SVD identification and control procedure is used. This is because directions corresponding to low steady-state gains  $\Lambda_{m,ii}(0)$  are not manipulated by the SVD controller, and the designing of the SVD controller to be robust tends to prevent overly large dynamic excursions in the manipulated variables. In cases where constraint handling is necessary, any of the well-established multivariable antiwindup procedures can be applied. This results in a simple controller implementation.

The authors expressed the opinion that the poor performance often reported for industrial sheet and film process control systems is most likely due to the signs of the model gains being incorrectly identified. All model gains cannot be determined with confidence due to the limited quantity of experimental data, the relatively high level of measurement noise, and the poor conditioning of large-scale sheet and film processes. This poses an inherent limitation on the performance achievable by any control algorithm applied to these processes. The best control algorithms will manipulate only in directions for which the signs of the gains are known with confidence.

Although the focus of this article was on sheet and film processes, the results have relevance to any process that can be represented in pseudo-SVD form, a comprehensive list of which appears in Featherstone (1995). Many of the identification and control concepts also have implications for more general large-scale processes, which constitute a subject of current study.

## Acknowledgments

Support from the DuPont Young Faculty Award is gratefully acknowledged.

## Literature Cited

- Andersen, H. W., and M. Kummel, "Evaluating Estimation of Gain Directionality: Part 1: Methodology," *J. Process Control*, **2**, 59 (1992a).
- Andersen, H. W., and M. Kummel, "Evaluating Estimation of Gain Directionality. Part 2: A Case of Binary Distillation," *J. Process Control*, **2**, 67 (1992b).
- Andersen, H. W., K. H. Rasmussen, and S. B. Jorgensen, "Advances in Process Identification," *Proc. Int. Conf. on Chemical Process Control (CPC-IV)*, Padre Island, TX, published by CACHE, Austin, TX (1991).
- Åström, K. J., U. Borisson, L. Ljung, and B. Wittenmark, "Theory and Application of Self-tuning Regulators," *Automatica*, **13**, 457 (1977).
- Åström, K. J., and B. Wittenmark, "On Self Tuning Regulators," *Automatica*, **9**, 185 (1973).
- Åström, K. J., and B. Wittenmark, *Computer Controlled Systems: Theory and Design*, Prentice Hall, Englewood Cliffs, NJ (1984).
- Balas, G. J., J. C. Doyle, K. Glover, A. K. Packard, and R. S. R. Smith,  *$\mu$ -Analysis and Synthesis Toolbox ( $\mu$ -Tools): Matlab Functions for the Analysis and Design of Robust Control Systems*, The MathWorks, Natick, MA (1992).
- Bergh, L. G., and J. F. MacGregor, "Spatial Control of Sheet and Film Forming Processes," *Can. J. Chem. Eng.*, **65**, 148 (1987).
- Bialkowski, W. L., "Application of Steady State Kalman Filters—Theory with Field Results," *Proc. Joint Autom. Control Conf.*, **17**, published by IEEE, Piscataway, NJ, 361 (1978).
- Bialkowski, W. L., "Application of Kalman Filters to the Regulation of Dead Time Processes," *IEEE Trans. Automat. Contr.*, **AC-28**, 400 (1983).
- Bialkowski, W. L., "Control Systems Engineering. Have We Gone Wrong? *InTech*, p. 27 (Feb. 1986).
- Boyle, T. J., "Practical Algorithms for Cross-direction Control," *TAPPI*, **61**, 77 (1978).
- Braatz, R. D., "Control of Sheet and Film Processes," *SIAM Conf. on Control and Its Applications*, Soc. Ind. Appl. Math., Philadelphia, PA (1995).
- Braatz, R. D., "Robustness Margin Computation for Large Scale Systems," AICHE Meeting, Chicago, IL (1996).
- Braatz, R. D., "The Average-case Identifiability of Large Scale Systems," AICHE Meeting, Los Angeles (1997).
- Braatz, R. D., B. A. Ogunnaike, and A. P. Featherstone, "Identification, Estimation, and Control of Sheet and Film Processes," *Proc. IFAC World Congress*, San Francisco, published by Elsevier Science Ltd., New York, p. 319 (1996).
- Braatz, R. D., M. L. Tyler, M. Morari, F. R. Pranckh, and L. Sartor, "Identification and Cross-directional Control of Coating Processes," *AICHE J.*, **38**, 1329 (1992).
- Braatz, R. D., and J. G. VanAntwerp, "Advanced Cross-directional Control," *Control Systems '96 Preprints*, Halifax, Nova Scotia, Canada, p. 15 (1996a).
- Braatz, R. D., and J. G. VanAntwerp, "Robust Cross-directional Control of Large Scale Paper Machines," *Proc. of the IEEE International Conf. on Control Applications*, Dearborn, MI, p. 155 (1996b).
- Braatz, R. D., P. M. Young, J. C. Doyle, and M. Morari, "Computational Complexity of  $\mu$  Calculation," *IEEE Trans. Automat. Contr.*, **39**, 1000 (1994).
- Brunk, H. D., *An Introduction to Mathematical Statistics*, 2nd ed., Xerox College Publishing, Lexington, MA (1965).
- Callari, J., "New Extrusion Lines Run Tighter, Leaner," *Plastics World*, p. 28 (Jan. 1990).
- Campo, P. J., and M. Morari, "Robust Control of Processes Subject to Saturation Nonlinearities," *Comput. Chem. Eng.*, **14**, 343 (1990).
- Campo, P. J., and M. Morari, "Achievable Closed Loop Properties of Systems Under Decentralized Control: Conditions Involving the Steady State Gain," *IEEE Trans. Automat. Contr.*, **AC-39**, 932 (1994).

- Cegrell, T., and T. Hedqvist, "Successful Adaptive Control of Paper Machines," *Automatica*, **11**, 53 (1975).
- Charrier, J.-M., *Polymeric Materials and Processing*, Oxford Univ. Press, New York (1991).
- Chen, S.-C., and R. G. Wilhelm, Jr., "Optimal Control of Cross-machine Direction Web Profile with Constraints on the Control Effort," *Proc. American Control Conf.*, Seattle, WA, published by IEEE, Piscataway, NJ, p. 1109 (1986).
- Chiang, R. Y., and M. G. Safonov, *Robust Control Toolbox: For Use with MATLAB*, The MathWorks, Natick, MA (1992).
- Cuffey, W. H., "Some Factors Involved in Basis Weight Uniformity," *TAPPI*, **40**, 190A (1957).
- Devore, J. L., *Probability and Statistics for Engineering and the Sciences*, Brooks/Cole Publishing, Monterey, CA (1982).
- Doyle, J. C., "Analysis of Feedback Systems with Structured Uncertainties," *IEE Proc. D*, **129**, 242 (1982).
- Dumont, G. A., "Application of Advanced Control Methods in the Pulp Paper Industry—A Survey," *Automatica*, **22**, 143 (1986).
- Featherstone, A. P., *Control Relevant Identification of Structured Large Scale Systems*, M.S. Thesis, Univ. of Illinois, Urbana (1995).
- Featherstone, A. P., *Control Relevant Identification of Large Scale Sheet and Film Processes*, PhD Thesis, Univ. of Illinois, Urbana (1997).
- Featherstone, A. P., and R. D. Braatz, "Control Relevant Identification of Sheet and Film Processes," *Proc. American Control Conf.*, Seattle, WA, published by IEEE, Piscataway, NJ, p. 2692 (1995).
- Golub, G. H., and C. F. van Loan, *Matrix Computations*, The Johns Hopkins Press, Baltimore, MD (1983).
- Grosdidier, P., M. Morari, and B. R. Holt, "Closed-loop Properties from Steady-state Gain Information," *Ind. Eng. Chem. Fundam.*, **24**, 221 (1985).
- Halouskova, A., M. Karny, and I. Nagy, "Adaptive Cross-direction Control of Paper Basis Weight," *Automatica*, **29**, 425 (1993).
- Heaven, E. M., T. M. Kean, I. M. Jonsson, M. A. Manness, K. M. Vu, and R. N. Vyse, "Applications of System Identification to Paper Machine Model Development and Controller Design," *IEEE Conf. on Control Applications*, IEEE, Piscataway, NJ, p. 227 (1993).
- Hensen, F., *Plastics Extrusion Technology*, Oxford Univ. Press, New York (1988).
- Hovd, M., R. D. Braatz, and S. Skogestad, "SVD Controllers for  $H_2$ ,  $H_\infty$ , and  $\mu$ -Optimal Control," *Automatica*, **33**, 433 (1996).
- Jacobsen, E. W., "Identification for Control of Strongly Interactive Plants," AIChE Meeting, San Francisco (1994).
- Jones, R. H., "Maximum Likelihood Fitting of ARMA Models to Time Series with Missing Observations," *Technometrics*, **22**, 389 (1980).
- Kan, C. E., "A New Caliper Control Actuator-evaluation Process and Practical Results," *TAPPI J.*, **70**(7), 81 (1987).
- Karlsson, H., and L. Haglund, "Optimal Cross-direction Basis Weight and Moisture Profile Control on Paper Machines," *Proc. Int. Pulp and Paper Process Control Symp.*, Vancouver, B.C., Canada (1983).
- Kajer, A. P., W. P. Heath, and P. E. Wellstead, "Identification of Cross-directional Behaviour in Web Production: Techniques and Experience," *Proc. IFAC Symp. on System Identification*, Copenhagen, Denmark, published by Elsevier Science Ltd., New York (1994).
- Koop, A., *Deformation einer elastischen flexlippe*, Bonn, Diplomarbeit, Bonn, Germany (1993).
- Koung, C. W., and J. F. MacGregor, "Design of Identification Experiments for Robust Control—A Geometric Approach for Bivariate Processes," *Ind. Eng. Chem. Res.*, **32**, 1658 (1993).
- Kristinsson, K., and G. A. Dumont, "Paper Machine Cross Directional Basis Weight Using Gram Polynomials," *Automatica*, **32**, 533 (1996).
- Laughlin, D., M. Morari, and R. D. Braatz, "Robust Performance of Cross-directional Basis-Weight Control in Paper Machines," *Automatica*, **29**, 1395 (1993).
- Li, W., and J. H. Lee, "Control Relevant Identification of Ill-conditioned Systems: Estimation of Gain Directionality," *Comput. Chem. Eng.*, **20**, 1023 (1994).
- Ma, M. S., and D. C. Williams, "A Simplified Adaptive Model Predictive Controller," *TAPPI J.*, **71**, 190 (1988).
- Martino, R., "Motor-driven Cams Actuator Flexible-lip Automatic Die," *Modern Plastics*, **68**, 23 (1991).
- Mhatre, S., and C. B. Brosilow, "Multivariable Model State Feed-back," *Proc. IFAC World Congress*, San Francisco, Vol. M, published by Elsevier Science Ltd., New York, p. 139 (1996).
- Morari, M., "Robust Stability of Systems with Integral Control," *IEEE Trans. Automat. Contr.*, **30**, 574 (1985).
- Morari, M., and E. Zafiriou, *Robust Process Control*, Prentice Hall, Englewood Cliffs, NJ (1989).
- Richards, G. A., "Cross Direction Weight Control," *Japan Pulp Paper*, p. 41 (Nov. 1982).
- Russell, E. L., and R. D. Braatz, "Analysis of Large Scale Systems with Model Uncertainty, Actuator and State Constraints, and Time Delays," AIChE Meeting, Chicago, IL (1996).
- Russell, E. L., C. P. H. Power, and R. D. Braatz, "Multidimensional Realizations of Large Scale Uncertain Systems for Multivariable Stability Margin Computation," *Int. J. Robust Nonlinear Control*, **7**, 113 (1997).
- Safonov, M. G., "Stability Margins of Diagonally Perturbed Multivariable Feedback Systems," *IEE Proc. D*, **129**, 251 (1982).
- Sikora, R. F., W. L. Bialkowski, J. F. MacGregor, and P. A. Tayler, "A Self-tuning Strategy for Moisture Control in Papermaking," *Proc. American Control Conf.*, San Diego, published by IEEE, Piscataway, NJ, p. 54 (1984).
- Skogestad, S., M. Morari, and J. C. Doyle, "Robust Control of Ill-Conditioned Plants: High Purity Distillation," *IEEE Trans. Automat. Contr.*, **AC-33**, 1092 (1988).
- Skogestad, S., and I. Postlethwaite, *Multivariable Feedback Control: Analysis and Design*, Wiley, New York (1996).
- Van den Hof, P. M., and R. J. P. Schrama, "Identification and Control—Closed-loop Issues," *Automatica*, **31**, 1751 (1995).
- Wallace, B. W., "Economic Benefits Offered by Computerized Profile Control of Weight, Moisture, and Caliper," *TAPPI*, **64**, 79 (1981).
- Wigostsky, V., "Extrusion," *Plastics Eng.*, **52**, 22 (1996).
- Wilhelm, R. G., Jr., and M. Fjeld, "Control Algorithms for Cross Directional Control," *Proc. IFAC PRP Conf.*, Antwerp, Belgium, published by Elsevier Science Ltd., New York, p. 163 (1983).
- Wilkinson, A. J., and A. Hering, "A New Control Technique for Cross Machine Control of Basis Weight," *Preprints IFAC PRP Conf.*, Antwerp, Belgium, published by Elsevier Science Ltd., New York, p. 151 (1983).
- Young, G. E., R. L. Lowery, and D. W. Plummer, "Longitudinal Dynamics of the Rewind Portion of a Web Handling Machine," *Proc. American Control Conf.*, published by IEEE, Piscataway, NJ, p. 1403 (1986).
- Zheng, A., M. V. Kothare, and M. Morari, "Antiwindup Design for Internal Model Control," *Int. J. Control*, **60**, 1015 (1994).

## Appendix: Proof of Theorem 1

The following lemmas are used to prove Theorem 1.

*Lemma 1.* Assume  $P(s) = U\Lambda(s)V^T$  and  $K(s) = V\Lambda_K(s)U^T$ . Then the closed-loop system is internally stable if and only if each SISO loop with  $\Lambda_{K,ii}(s)$  and  $\Lambda_{ii}(s)$  is stable.

*Lemma 2.* Assume  $g(s) = \tilde{g}(s)/s^r$ , where  $\tilde{g}(s)$  is stable. Then the closed loop system with  $g = pk$  is stable only if  $\tilde{g}(0) > 0$ .

*Proof of Lemma 1.* The MIMO system is internally stable if and only if

$$\begin{bmatrix} PK(I + PK)^{-1} & (I + PK)^{-1}P \\ K(I + PK)^{-1} & -K(I + PK)^{-1}P \end{bmatrix} \quad (A1)$$

is stable. With the pseudo-SVD decompositions of  $P$  and  $K$ , Eq. A1 is equivalent to the condition that

$$\begin{bmatrix} U\Lambda\Lambda_K(I + \Lambda\Lambda_K)^{-1}U^T & U(I + \Lambda\Lambda_K)^{-1}\Lambda V^T \\ V\Lambda_K(I + \Lambda\Lambda_K)^{-1}U^T & -V\Lambda_K(I + \Lambda\Lambda_K)^{-1}\Lambda V^T \end{bmatrix} \quad (A2)$$

is stable. Pre- and postmultiplication by unitary matrices does not affect the stability of Eq. A2, so the MIMO system is internally stable if and only if

$$\begin{bmatrix} \Lambda_{ii}(1 + \Lambda_{ii}\Lambda_{K,ii})^{-1} & (1 + \Lambda_{ii}\Lambda_{K,ii})^{-1}\Lambda_{ii} \\ \Lambda_{K,ii}(1 + \Lambda_{ii}\Lambda_{K,ii})^{-1} & -\Lambda_{K,ii}(1 + \Lambda_{ii}\Lambda_{K,ii})^{-1}\Lambda_{ii} \end{bmatrix} \quad (\text{A3})$$

is stable for all  $i$ , which occurs if and only if each SISO loop with  $\Lambda_{ii}$  and  $\Lambda_{K,ii}$  is stable for all  $i$ .

*Proof of Lemma 2.* The proof is similar to the proof of a result in Morari (1985). The transfer function  $\tilde{g}(s)$  can be written as  $\tilde{g}(s) = n(s)/d(s)$  with

$$d(s) = s^q + \dots + d(0). \quad (\text{A4})$$

Then  $\tilde{g}(s)$  stable implies that

$$d(0) > 0 \quad (\text{A5})$$

from the Routh Criterion, and

$$\frac{1}{1 + g(s)} = \frac{s^r d(s)}{s^r (s^q + \dots + d(0)) + \dots + n(0)} \quad (\text{A6})$$

stable, implies that

$$n(0) > 0, \quad (\text{A7})$$

also from the Routh Criterion. Conditions of Eqs. A5 and A7 imply that  $\tilde{g}(0) > 0$ .

*Proof of Theorem 1.* (1) As a result of Lemma 1,  $K(s) = V\Lambda_K(s)U^T$  stabilizes both  $P_t(s)$  and  $P_m(s)$  if and only if each SISO loop with  $\Lambda_{K,ii}(s)$  and  $\Lambda_{t,ii}(s)$  is stable, and with  $\Lambda_{K,ii}(s)$  and  $\Lambda_{m,ii}(s)$  is stable, for all  $i$ . A necessary condition for this (Lemma 2 applied to these SISO loops) is that  $\tilde{\Lambda}_{K,ii}(0)\tilde{\Lambda}_{m,ii}(0) > 0$ , and  $\tilde{\Lambda}_{K,ii}(0)\tilde{\Lambda}_{t,ii}(0) > 0$ , for all  $i$ . This implies that  $\tilde{\Lambda}_{m,ii}(0)/\tilde{\Lambda}_{t,ii}(0) > 0$ , for all  $i$ , which is equivalent to  $\Lambda_{m,ii}(0)/\Lambda_{t,ii}(0) > 0$ , for all  $i$  [because  $P_t(s)$  and  $P_m(s)$  are stable].

(2) Assume that if  $\Lambda_{m,ii}(0)/\Lambda_{t,ii}(0) > 0$  for all  $i$ . Then there exists  $\gamma^* > 0$  sufficiently small [from Morari, (1985)] so that  $\Lambda_{K,ii}(s) = (\gamma^*/s)$  will stabilize each SISO loop, and will continue to do so for all  $0 < \gamma < \gamma^*$ . [Apply Morari (1985) to each  $\Lambda_{m,ii}(0)$  and  $\Lambda_{t,ii}(0)$ , and take the smallest  $\gamma^*$ .] Then Lemma 1 implies that  $K(s) = V\Lambda_{K,ii}(s)U^T$  is an integral SVD controller, which stabilizes both  $P_m(s)$  and  $P_t(s)$ .

*Manuscript received Aug. 9, 1996, and revision received Apr. 14, 1997.*